Title

Full-Rate AMR over DQPSK.

Source

James P. Seymour
Lucent Technologies
Network Wireless Systems
67 Whippany Rd. Rm. 2A-246
(973)-386-8096 (v)
(973)-386-6814 (f)
jpseymour@lucent.com

Andrea M. Tonello
Lucent Technologies
Network Wireless Systems
67 Whippany Rd. Rm. 1A-210

Keith Conner
Lucent Technologies
Network Wireless Systems
67 Whippany Rd. Rm. 14B-413
(973)-386-4358
(973)-386-6814 (f)
Faolk@lucent.com

Abstract

Currently there is an effort in place to standardize the AMR codec for TDMA6. In addition to this effort, the standardization of AMR over full-rate channels is also being considered. While 8-PSK modulation provides enough bits for enabling higher vocoding rates and potentially 6 users in a single 30 kHz channel (TDMA6), DQPSK has some advantages in terms of equalizer complexity (for dispersive channels), robustness and lower Peak-to-Average and Peak-to-Minimum ratios. Investigations comparing the performance of full-rate AMR with 8-PSK modulation and full-rate AMR with QPSK modulation indicated that there were advantages using 8-PSK. This contribution shows that it is possible to improve the performance of QPSK using DQPSK modulation with Iterative Decoding. Based on these new results and other advantages of DQPSK just mentioned, it is recommended that full-rate AMR be defined with DQPSK modulation in addition to 8-PSK modulation.

Recommendation

Review and adopt full-rate AMR over DQPSK.

Copyright

Introduction

This contribution considers the performance of DQPSK with Iterative Decoding for full-rate AMR. Iterative Decoding (ID) originally was exploited in turbo-codes. Assuming concatenated codes are used in the encoding stage, the output of the second of the two decoders is fed back into the first decoder in an iterative fashion. This has shown to provide substantial gains. With DQPSK, differential encoding followed by convolutional encoding can be thought of as concatenated codes and thus iterative decoding can be used to improve performance. Unfortunately, 8-PSK does not apply differential encoding and thus the use of iterative decoding for 8-PSK will provide no benefit. This leads to the performance of 8-PSK and DQPSK with ID being quite similar. This contribution explores the performance of DQPSK with ID for the 7.4 kbps vocoder and discusses some of the advantages of DQPSK with ID for AMR.

Theory of Iterative Decoding

The theory behind the use of iterative decoding for IS-136 is based on [1]. For ease of discussion, some of the concepts in [1] are repeated here.

1 System model

Consider a communication system model as in Figure 1. The information bit sequence, belonging to a given user, is represented by b_i, $i=0,\ldots,N_b-1$. The information bits are first channel encoded (bits c_i , $i=0,\ldots,N_c-1$) with a rate k/n convolutional code, not necessarily recursive-systematic, interleaved (bits d_i , $i=0,\ldots,N_d-1$, $N_d=N_c$), and then M-DPSK modulated to produce the symbol sequence x_i , $i=0,\ldots,N_k-1$ with $N_k=N_d/log_2M$. It should be noted that for ease of notation the same time indices i are used in each variable. The complex symbols x_i, transmitted at rate $1/T$, after pulse shaping, are RF modulated. This signal then propagates through either a time-non-dispersive or a time-dispersive noisy fading channel. Thus, the channel may introduce intersymbol interference. Co-channel interference signals, if present, undergo the same operations.

A receiver with an antenna array of N_a elements captures such signals (Figure 2). After RF demodulation and matched filtering, the base-band signals $y_a(t)$ at each antenna a are sampled at rate $1/T$. We model the sequence $y_a(kT)=y_{a,k}$ of N_k complex samples at each antenna a , with a discrete time transversal filter:

$$y_{a,k} = \sum_{l=0}^{N_t-1} h_{a,k,l}\, x_{k-l} + y_{a,k}^{\text{int}} + n_{a,k} \qquad (1)$$

where N_t is the number of taps in the FIR model.

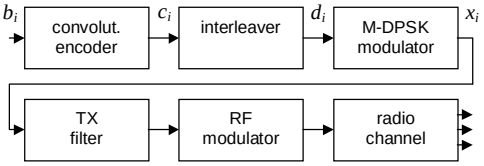

Figure 1: Communication system model.

The equivalent multiplicative channel state information (CSI) is represented by $h_{a,k,l}$. We model $h_{a,k,l}$ as statistically independent over index a complex Gaussian variables. Their amplitude is Rayleigh distributed, and their time correlation (i.e. over index k) is given by $\Omega_{a,l}J_0(2\pi f_d kT)$, where $f_d=vf_c/c$ ($J_0(.)$: zero-order Bessel function, v: mobile speed, f_c: carrier frequency, c: speed of light). The co-channel interference and AWG thermal noise are respectively given by $y_{a,k}^{\text{int}}$ and $n_{a,k}$ (overall by $w_{a,k}$). Equation (1) can be concisely rewritten in matrix form as:

$$\underline{\underline{y}} = \underline{\underline{h}}\,\underline{\underline{x}} + \underline{\underline{w}} \tag{2}$$

where $\underline{\underline{y}}$ is a N_a x N_k matrix. In Figure 2, $\underline{y}_i$ represents a vector of N_a samples taken at time iT.

2 Iterative receiver structure

The receiver task is to determine the transmitted information bit sequence b_i. A two-stage receiver can accomplish such a goal. The first stage (detector) computes reliability information on the coded bits d_i from the channel observations $\underline{y}$. The reliability information is given by the log-likelihood ratios $L(d_i)=ln[P(d_i=+1)/P(d_i=-1)]$ (referred to as L-values [6]). The second stage (decoder), after deinterleaving, performs decoding using the values calculated in the first stage.

We consider generation of optimum L-values in the first stage by application of the MAP algorithm [2]. The MAP algorithm can exploit the memory possessed by an M-DPSK signal that propagates through either a time-non-dispersive or a time-dispersive channel. Better L-values can be generated if the a priori probabilities of the coded bits are known. Such a priori probabilities can be estimated by the second stage (i.e. channel decoder) if a soft output decoder is deployed. The resulting receiver (Fig. 2) has a structure similar to the one originally proposed for decoding of turbo codes [5]. Thus, the detector computes a posteriori L-values for the coded bits $L(d_i|\underline{y})$ from only the channel observations, at the first iteration. These L-values are deinterleaved and fed to the decoder. The decoder (based on the MAP algorithm) computes L-values for both the information bits, $L(b_i)$, and for the coded bits, $L(c_i)$, by exploiting the memory of the convolutional code. The L-values $L(c_i)$ are used to derive an estimate of the a priori L-values of the coded bits $L_a(d_i)$ through the relation:

$$L_a(d_i) = \text{intlv}\left[L_e(c_i)\right] = \text{intlv}\left[L(c_i) - L_a(c_i)\right] \tag{3}$$

In equation (3) we attempt to minimize the correlation between the estimated a priori information and previous calculated information by feeding back only extrinsic information, $L_e(c_i)$ (i.e. incremental soft-decision information) [5]. The a priori L-values $L_a(d_i)$ can be used in a new detection iteration for refining the a posteriori L-values $L(d_i|\underline{y})$. Similarly, extrinsic information $L_e(d_i)$ is computed at the output of the detector and is fed to the decoder for a new decoding iteration. After the final iteration, hard decisions on $L(b_i)$ yield the decoded information sequence.

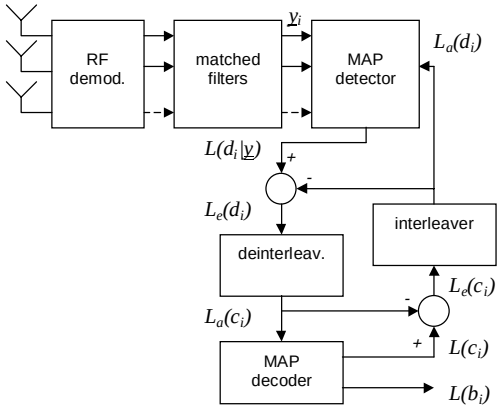

Figure 2: Iterative receiver with multiple antennas.

As it is shown in Section 5 multiple iterations can give significant performance gains. The steps involved in the MAP algorithm [2],[3],[4] are discussed in the next section. In particular, generation of a posteriori L-values $L(d_i|\underline{y})$ is addressed when the modulation is M-DPSK and the channel is either time-non-dispersive or time-dispersive in the presence of spatially correlated noise.

3 MAP detection of M-DPSK signals

See [1] for a detailed discussion of the optimum MAP detection scheme for M-DPSK signals.

4 Application to IS-136 TDMA

In this section, we investigate the applicability of the suggested receiver to the IS-136 TDMA system [6]. The North American TDMA digital traffic channel (DTC) uses $\pi/4$-DQPSK modulation with Gray mapping, and a memory 5, rate ½ (with 8 bits puncturing) tail terminated convolutional code. The coding scheme with the ACELP vocoder is shown in Figure 3. We depict in Figure 4 the operations that take place every 20 ms.

A speech frame $\underline{b}$ of 148 information bits is partitioned into 3 sub-blocks or classes (see also Fig. 3): 52 C2 bits, 48 C1B bits, and 48 C1A bits. After adding 7 CRC bits to C1A, the C1A+C1B=C1 bits are convolutional encoded, while C2 bits are left uncoded. This generates a block $\underline{c}$ of 260 bits that are first reordered with a 26 by 10 matrix interleaver and then chain interleaved across 2 slots (20 ms apart). Thus, at a given transmission time interval, the 130 bits $\underline{d1}$ belong to the previous encoded speech frame, while the 130 bits $\underline{d2}$ belong to the current encoded speech frame. These bits together with other non-data bits, are slot formatted (Figure 5, considering the uplink) and modulated in order to generate blocks of symbols $\underline{x}$. The symbols are transmitted at rate 24.3 kbauds. Pulse shaping is obtained with a root raised cosine filter with roll-off=0.35.

As a result of chain interleaving, the input L-values $L_a(\underline{c})$ to the decoder are obtained from MAP detection of at least two slots. In turn, only partial amounts of soft information can be fed back from a given decoder to a given detector. Even though it is not the only solution, our receiver implementation (Figure 4) requires MAP detection over two consecutive received slots (20 ms apart), and MAP convolutional decoding over one encoded speech frame per iteration. Since only C1 bits are convolutionally encoded, only the a priori L-values of coded C1 bits are fed back from a given decoder. Thus, at the first iteration MAP detection over a slot takes place setting to zero the a priori L-values of coded C1 and C2 bits. In successive iterations, MAP detection over a slot is run using the observations and the a priori L-values of coded C1 bits generated from the decoder outputs (according to (3)).

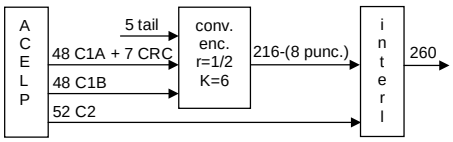

Figure 3: Coding scheme in IS-136 DTC.

It should be noted that the feedback receiver in Figure 4 doesn't introduce any extra processing delay, as otherwise would be the case if we increased the number of slots and/or encoded speech frames processed at each iteration. This would allow augmentation of the amount of feedback information to each processed slot.

Finally, simulations show that the proposed iterative receiver achieves significant BER gains in all classes, both C1 and C2, even though C2 bits are not convolutionally encoded (see next section).

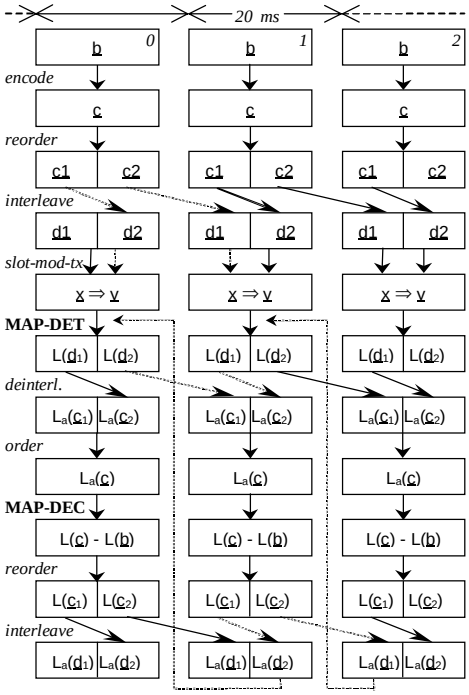

Figure 4: IS-136 processing with feedback.

gt	rt	data	sync	data	sacch	cdvcc	data
6	6	16	28	122	12	12	122

Figure 5: Slot format in IS-136 TDMA uplink.

Performance Results

In this section, several coding schemes using DQPSK modulation and 8-PSK modulation for TDMA3 Full Rate Voice Applications using a 7.4 kbits/s vocoder are compared.

In particular the following parameters and coding schemes are considered:

1) Acelp vocoder at 7.4 kbits/s. Class partition as follows: 48 C1A + 7 CRC + 48 C1B + 52 C2 bits.

2) DQPSK with 260 payload bits. Coding scheme as in IS-136. Thus C1A+CRC+C1B are coded with a memory 5, tail terminated, rate 1/2 convolutional code. C2 bits are left uncoded.

3) 8-PSK with 390 payload bits. C1A+CRC+C1B coded with a memory 5, tail terminated, rate 8/25 convolutional code. C2 bits are left uncoded. We refer to this scheme as 8-PSK S1.

4) 8-PSK with 390 payload bits. C1A+CRC+C1B+C2 all coded with a memory 5, tail terminated, rate 16/39 convolutional code. We refer to this scheme as 8-PSK S2.

Perfect channel knowledge is assumed. Iterative decoding as described in the previous section is applied to DQPSK with up to 3 extra iterations. Ideal coherent detection is applied to 8-PSK. Note that iterative decoding yields similar performance with 1 and 3 extra iterations.

Simulation results are reported for a flat Rayleigh fading channel with maximum Doppler spread equal to 10 Hz and 100 Hz. The number of simulated frames is set to 10000. In Figs. 6-9 we report C1A FER and C2 BER.

The simulation results can be summarized as follows:

A) At 10 Hz Doppler, 8-PSK S1 performs about 2 dB better in C1A FER and 3 dB better in C1B BER over DQPSK. However, 8-PSK S1 is 5 dB worse in C2 BER. Note that iterative decoding gives small improvements in C1 performance with extra iterations (i.e. using feedback). This is due to the fact that the weak interleaver is not able to decorrelate successfully the errors introduced by the bursty channel.

B) At 10 Hz Doppler, 8-PSK S2 performs about 1 dB worse in C1A FER and about 1 dB better in C1B BER over DQPSK. Furthermore since all C1B and C2 bits are coded, 8-PSK S2 performs about 4 dB better in C2 BER than DQPSK.

C) At 100 Hz Doppler, 8-PSK S1 performs about 1 dB better in C1A FER and 3 dB better in C1B BER compared to DQPSK. Again, 8-PSK S1 is 5 dB worse in C2 BER.

D) At 100 Hz Doppler, 8-PSK S2 performs about .5 dB worse in C1A FER and about .5 dB better in C1B BER compared to DQPSK. 8-PSK S2 performs much better in C2 BER since C2 bits are coded.

It is likely that unequal error protection would be used instead of equal error protection (S2) for 8-PSK. This would improve the C1A FER for 8-PSK S2 and degrade the C2 BER. This would lead to similar C1A FER and C1B BER performance for 8-PSK S2 and DQPSK with ID, but would still likely leave some advantage in C2 BER for 8-PSK S2.

Although 8-PSK is likely to show advantages in C2 BER, there are some advantages for DQPSK with ID. First, DQPSK with ID allows for a much lower complexity equalizer to be implemented for large delay spread environments. Clearly, a 2 tap equalizer for 8-PSK would requires 8x8=64 states, whereas for DQPSK requires 4x4=16 states. Assuming one additional iteration for ID leads to a DQPSK equalizer of about half the complexity of an 8-PSK equalizer. Larger tap equalizers lead to even bigger complexity savings for DQPSK.

Second, ideal coherent detection was assumed in the above results. Since the performance of the 8-PSK algorithm relies heavily on proper channel estimation, it is believed that in practical systems the performance of 8-PSK will degrade more than DQPSK with ID.

Third, DQPSK is expected to be more robust than 8-PSK against other degradations not included in the simulations (e.g. EVM, Freq. Offset, Symbol Timing Offsets, etc.). These impairments are much more likely to degrade 8-PSK performance more than DQPSK performance.

Finally, 8-PSK modulation requires larger Peak-to-Average Ratio (PAR) and Peak-to-Minimum Ratio (PMR) than DQPSK. This puts an added burden on amplifiers are for 8-PSK modulation than for DQPSK modulation.

Although this contribution has only considered performance of the 7.4 kbps vocoder, similar performance is expected for the vocoder rates less than 7.4 kbps. The performance of DQPSK with ID for higher vocoder rates is for further study. Based on the noted advantages of DQPSK, it is recommended that full-rate AMR be defined not only over 8-PSK but also over DQPSK modulation in order to realize these advantages.

Conclusions

This document has presented results of DQPSK with Iterative Decoding (ID) using the 7.4 kbps vocoder. Performance of DQPSK with ID is similar to 8-PSK performance in terms of C1A FER and C1B BER. 8-PSK has the advantage of being able to code all the bits and thus not having any C2 bits. However, the advantages of DQPSK are that equalization can be performed at much lower complexity, DQPSK is more robust against other impairments (e.g. EVM, Freq. Offset, Timing Offset), DQPSK is most robust against channel estimation errors, and DQPSK has lower Peak-to-Average and Peak-to-Minimum characteristics. Due to these advantages of DQPSK, it is recommended that full-rate AMR be defined over DQPSK modulation in addition to full-rate AMR over 8-PSK modulation. AMR vocoder rates greater than 7.4 kbps that could be supported with DQPSK is for further study.

References

[1] A. Tonello, "Iterative MAP detection of M-DPSK coded signals in fading channels with application to IS-136 TDMA", IEEE VTC 1999 Fall Amsterdam, September 1999, pp. 1615-1619.

[2] L.R. Bahl, J. Cocke, F. Jelinek, J. Raviv, 'Optimal decoding of linear codes for minimizing symbol error rate'. *IEEE Tr. Info. Theory, March 1974*, pp. 284-287.

[3] J. Hagenauer, E. Offer, L. Papke, 'Iterative decoding of binary block and convolutional codes', *IEEE Tr. Info Theory, March 1996*, pp. 429-445.

[4] A.J. Viterbi, 'An intuitive justification and a simplified implementation of the MAP decoder for convolutional codes', *IEEE JSAC February 1998*, pp. 260-264.

[5] C. Berrou, A. Glavieux, P. Thitimajshima, 'Near Shannon limit error correcting coding and decoding: turbo codes'. *ICC 1993*, pp. 1064-1070.

[6] TIA/EIA IS-136.2 standard, December 1994.

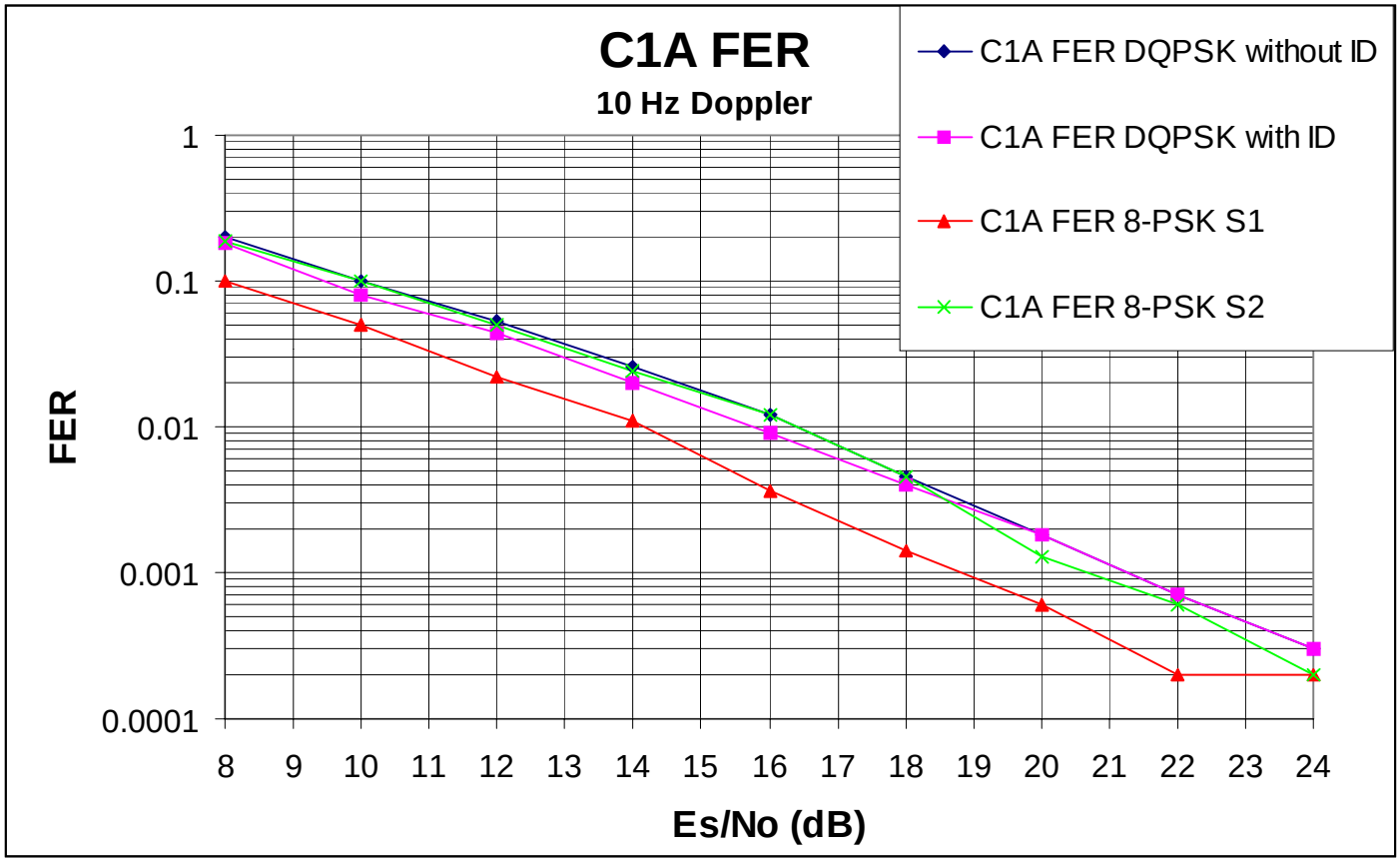

Figure 6. C1A FER Performance of DQPSK, DQPSK with ID, 8-PSK S1 and 8-PSK S2 at 10 Hz Doppler.

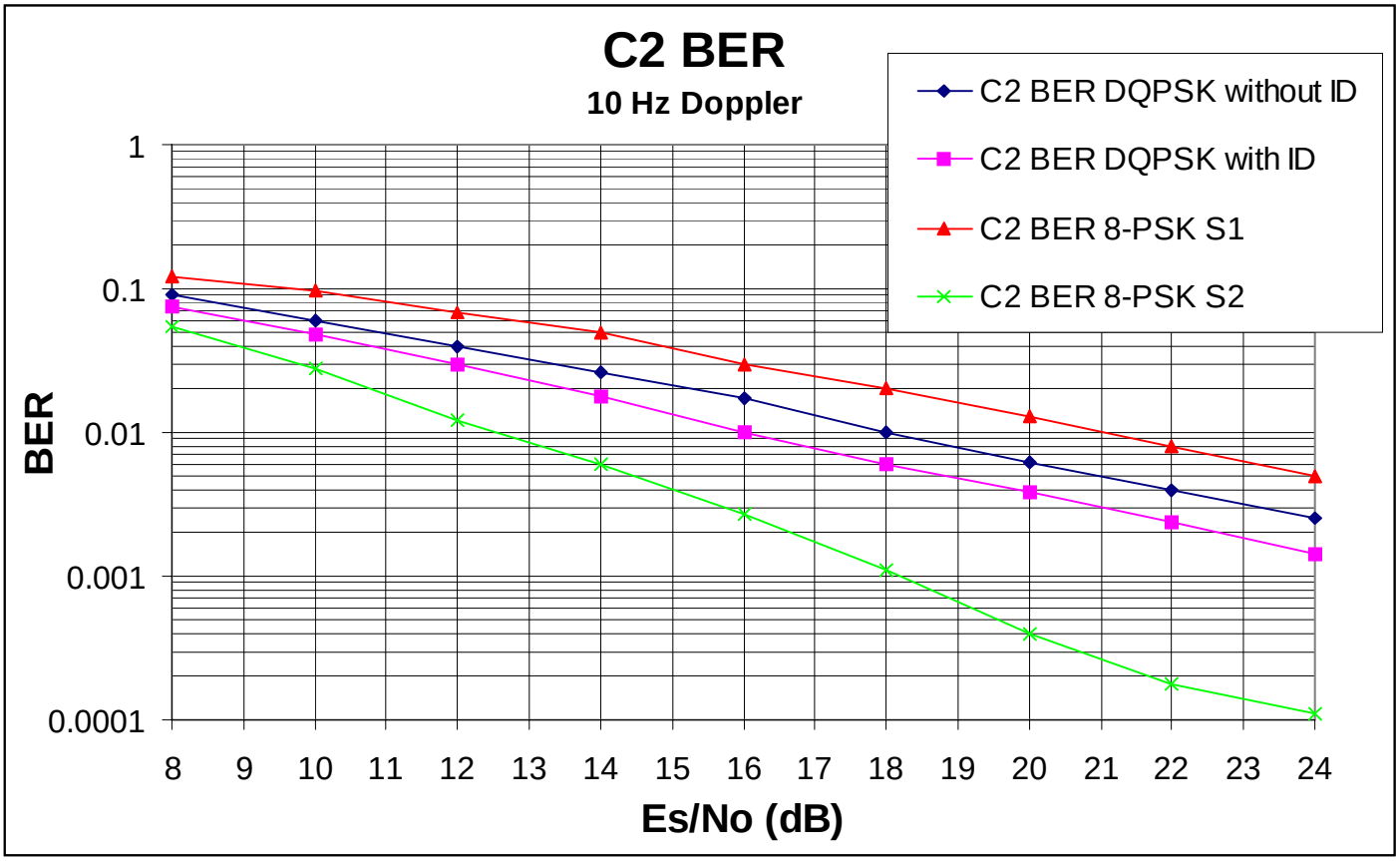

Figure 7. C2 BER Performance of DQPSK, DQPSK with ID, 8-PSK S1 and 8-PSK S2 at 10 Hz Doppler.

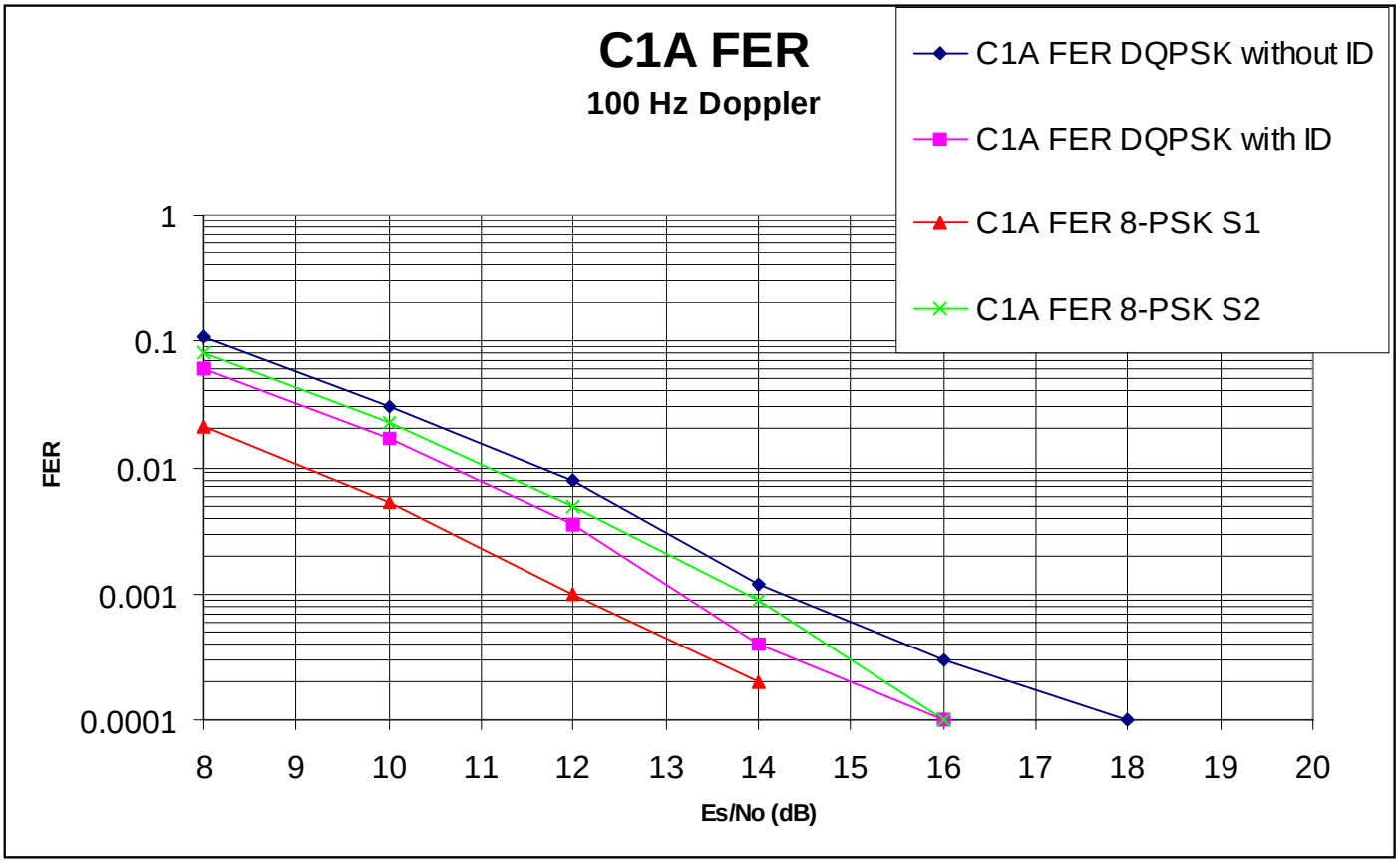

Figure 8. C1A FER Performance of DQPSK, DQPSK with ID, 8-PSK S1 and 8-PSK S2 at 100 Hz Doppler.

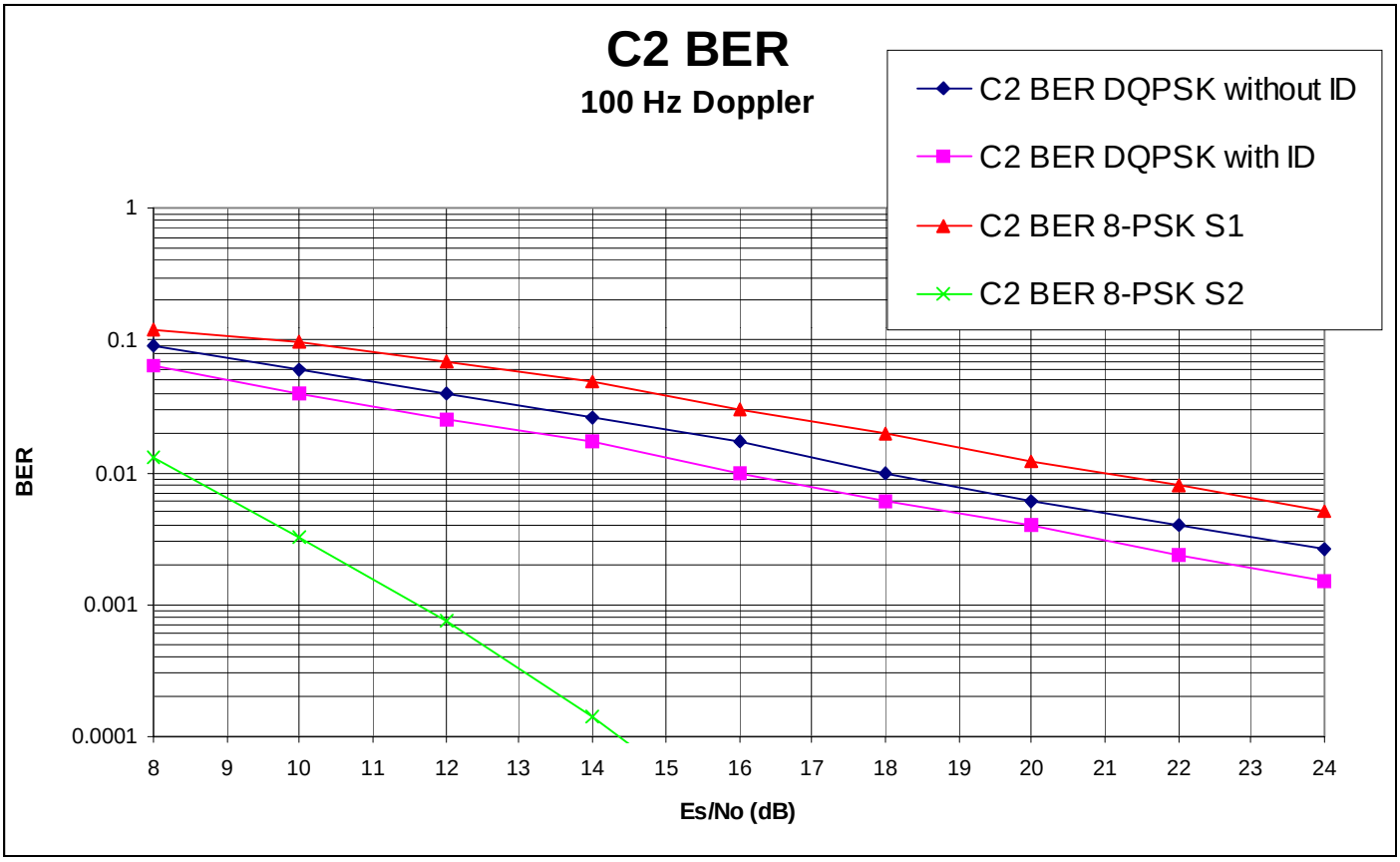

Figure 9. C2 BER Performance of DQPSK, DQPSK with ID, 8-PSK S1 and 8-PSK S2 at 100 Hz Doppler.